6. Russakovsky, O. et al. 2014. “ImageNet Large Scale Visual Recognition Challenge.” International Journal of Computer Vision. http://link.springer.com/article/10.1007/s11263-015-0816-y#
7. Hochreiter, Sepp, and Jürgen Schmidhuber. 1997. “Long Short-Term Memory.” Neural Computation, 9(8):1735–1780. ftp://ftp.idsia.ch/pub/juergen/lstm.pdf
8. Graves, Alex. 2014. “Generating Sequences With Recurrent Neural Networks.” http://arxiv.org/abs/1308.0850

LUNG REGION SEGMENTATION BASED ON COMPUTER TOMOGRAPHIC IMAGES

Nadine Suzanne Francis
Supervisor: Sergey V Axyonov
(National Research Tomsk Polytechnic University)
e-mail: nadinesuzannefrancis@gmail.com

Abstract. The article is written for the benefit of hospitals in order to identify segments of the lungs and thereby help in the process of bisecting lungs according to their respective segments during surgery. Further research in this area can also help in identification of various abnormalities related to each segment and also identify abnormal walls of unhealthy lungs. Segmentation of the lungs has not been implemented in reality, as the lung, being an organ with dynamic chest volumes during respiratory cycles, makes it impossible to address changes during respiration unlike fixed structures like the brain. Further, abnormalities situated on the walls of lung segments, make it more difficult to address volume changes concerned with the lungs. The author of this paper has provided a more effective method to identify various lung segments by using various well known segmentation techniques combined together to identify moving lung image segments more effectively.

Key words: lung segmentation, ct images on organs, segmentation methods, study of lung imaging, abnormalities in lung segments, combined segmentation.

Introduction. In computer tomography related to cardio-vascular system, high resolution computer tomography (HRCT) is used, which in turn helps to diagnose diseases that cannot be or is difficult to detect through physical examination, such us tumours, cancer, pneumonia, etc [1]. When the lung has a high density of pathologies, it becomes even more difficult to segment it as it becomes more difficult to detect its different segments and also more difficult to detect the borders of various segments.

Detection and segmentation must be performed with even more accuracy, because elimination of any intricate detail in any of the images can lead to fatal results. It can even lead to the death of the patient, if some pathology that had to be detected was carelessly eliminated while attempting to segment the lungs.

In the past, segmentation of the lungs was carried out manually from the inputs provided by the radiologists who have expertise in diagnosing anatomic boundaries and lung pathologies [1, 2]. Due to the progress of software and computational efficiency in recent times, lung segmentation could be carried out automatically instead of manual intervention. Currently, single lung segmentation methods cannot be used as it is not improvised enough to accurately segment the lungs. Clinically these methods have not been used as their efficiency is not enough to take the risk of using them in hospitals. Most of the methods that exist use a particular subset to identify abnormalities in images. However, they usually fail to identify lesions in the lung or near the lung. They also fail in accuracy and computational efficiency.

Medical Image Segmentation usually occurs by incorporating object recognition where we understand everything related to images and also the details connected with the image which could be easily performed computationally with proper user interaction, and object delineation where the boundaries of the object are identified [3]. Delineation is almost impossible as it is difficult to identify the total spatial extent of the lung. Most of the segmentation processes that have been identified

for the lungs, work well only when the availability of attenuations present is little or none. These methods are very effective in calculating the volume of lungs with the initiation of computer- aided detection systems. But in extreme cases where pathological conditions are existent, those segmentation methods fail to perform efficiently. In other words, consolidation and cavities lead to inaccurate boundary identification. Moreover, the availability of pneumothorax or pleural effusion on an image provides extremely distorted results which in turn lead to incorrect quantification of the lungs.

The most widely used segmentation methods that provided good segmenting results with less abnormal lungs are region-based, neighboring anatomy-guided, threshold-based, shape-based and machine learning based.

Though these methods provide fairly good results with lungs that are in almost good condition, the don't do fairly well when the lung is affected. The efficacy of efficiency for a daily well-functioning lung [4] is given as follows.

$$DSC(V_{GT},V_{test}) = 2 \mid \underline{V_{GT} \frown V_{test}} \mid$$
$$\mid V_{GT} \mid + \mid V_{test} \mid$$

where V_{GT} is standard segmentation and V_{test} is segmentation using a method. The intersection determines the overlapping area between the reference standard and the test segmentation.

The Haussdorf distance [4] is also used to determine the distance between two boundaries to analyze the similarities between real and images segmented through these methods. These values proved that the method may have sensitivity less than 50%.

Sensitivity and specificity are also used to evaluate accuracy of segmentation [5]. Sensitivity is used measure the ratio of actual positives that are identified correctly to all positives. Any false positive identified incorrectly are called false negative. Sensitivity is calculated for false positives as follows:

$$Sensitivity = TP/P = TP/ (TP + FN).$$

where FN denote the false negatives. Specificity is used measure the ratio of the negatives that are correctly identified to all negatives. Specificity for false negatives is calculated as follows:

$$Specificity = TN/N = TN/ (TN + FP)$$

where FP denotes false positives, or incorrectly identified positives. A perfect segmentation should be 100% sensitive and 100% specific. Unfortunately, existing methods do not provide this value.

Methods and procedures used in segmenting the lungs. Most of the methods that have been described for segmentation and those which are clinically used today, though effective in segmenting the lungs have not been successful in identifying segments of the lungs but rather well defined features that exist in them. The author used methods to help in identifying the lung structure and eradicating unwanted elements from the lungs, thus illuminating a few of the lungs segments. In this work, first the border of the lungs are detected using Canny Method [6] and noise is filtered out using the median filter. Using the median filter on Canny Detected Images tends to highlight the noise alone and remove every other feature of the lungs. Hence the Canny Detected Image and the Median filtered image [7] are subtracted from each other to remove the noise. Finally an Erosion filter is used to remove veins or shorter neighbouring pixels and leave only lines that join the lung borders thus providing us a clear image of the lung segments. For lungs with disabilities or huge particles in it, a Blob filter could also be used to filter out these huge particles.

The functioning of each method is broken down below to understand how each visible segment of the lung is identified and highlighted. Though it did not provide all lung segments it managed to identify segments that were at the least visible to the human eye.

Canny Edge Detection was the first method used to eliminate unwanted features of the lung image and only identify all the prominent edges. To perform this operation, the lung image undergoes detection - where all real edge points being detected are maximized or increased in intensity. The processed image then undergoes localization - where real and detected edges should be approximately equal to each other and finally, the lung image undergoes identifying the number of respons-

es - where a real edge provides no more than one detected edge. This method uses Canny's mathematical formula known as 'Calculus of Variations'.

Figure 1: Diagrammatic Representation of Canny Detection Algorithm

Noise is first removed from the image using a Gaussian Filter. The gradient intensity of the result is then determined, which then undergoes non maximum suppression. Potential edges are then determined using the Direct threshold. Hysterisis is Applied to identify the edges for Canny.

The Canny detected lung image then undergoes median filtering which is a non linear filter

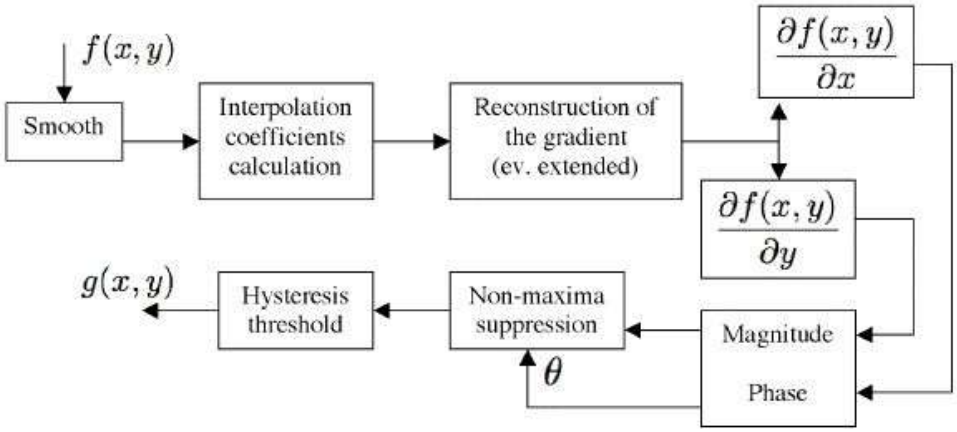

which intern removes all unwanted spots or noise from the lung image without eradicating the edges of the lung image. It works by moving through the image pixel by pixel and replacing each value with the median value of its neighbouring pixels. The pattern created by its neighbours is called "window", which slides pixel by pixel over the entire image. The median value is calculated by first sorting all the pixel values from the window in numerical order, and then replacing the pixel being considered with the median pixel value.

The median filter replaces a pixel by the median [8] or the middle value instead of the average value of all pixels in the neighbourhood ω,

$$y[m, n] = \text{median}\{x[i, j], (i, j) \varepsilon \omega\}$$

where ω represents a neighbourhood pixel which is defined by the user and is centered around the location [m, n] in the image. During filtering, the neighbouring pixels are ranked according to their intensity [7, 8] and the median value becomes the new value for the central pixel.

The main problem with median filters [4, 9] is they tend to erase the line that is narrower than half the width of neighbourhood lines and corners can also be rounded off. In order to prevent such errors, hybrid median filters are preferred. These filters are a three step ranking process that uses 2 subgroups of 5 x 5 neighbouring pixels. These subgroups are usually got from pixels that a parallel to the frame edges and form an angle of 45 degrees to the edges and are also centered to the reference pixel.

The median of a subgroup of pixels is determined. Then these two values are compared to the original pixel value. The median for these three values are then determined and is taken as the output pixel value. If a pixel contains a large neighbourhood, additional subgroup orientations are defined. The median filter however only detects the noise of the Canny filtered lung image and displays this noise as both are edge detecting algorithms.

The difference between the noise image and the canny filtered image is then calculated by identifying the difference between corresponding pixel color components of the two images. The resulting values from performing these calculations represent a single image without the noise factor. The extent of eliminating noise mainly depends on the image retrieved from median filtering and the difference algorithm that is applied between the two images.

The two images are taken and their pixels are compared by subtracting the pixels of the median filtered image from the CT lung image. Once all the same pixels are eliminated, a lung image with minimal noise is obtained.

Finally the output image from the previous stage is taken and passed through the erosion filter so that only the segments of the lung image is detected and the output is provided. Erosion and dilation methods are a part of morphological operations. It was originally developed only for binary images and later extended to grayscale images [10]. It mostly deals with describing shapes using sets.

Morphological operations use a structuring element S to interact with an image, thus being able to interact with an image thus the use of mathematical operations [11]. The structuring element is usually small when compared with the image. In the case of digital images, simple structuring binary elements are used which includes crosses and squares. In binary images, bright pixels are given high grey values and dark pixels end up with low grey values. Object pixels [11, 12] take the grey value 1 and are displayed as black whereas background pixels take the value 0 and appear as white. This helps in enhancing the clarity of binary images.

The structuring element S is defined as follows to create a more intuitive effect: The structuring element can be placed anywhere in the image. If the structuring element hits the set, the origin of the structuring element is part of the dilated set.

If the structuring element is not symmetrical, then the transpose of the element [12] is used in the procedure mentioned above. The transpose of the element is nothing but the structuring element mirrored in the origin:

$$S = \{s| (-s) \in S\}$$

Erosion ε(X) of a set X with structuring element S is given by the following formula

$$\varepsilon(X) = \{x|\forall s \in S, x + s \in X\}$$

Using the relation between sets and images, formulas for erosion ε and dilation δ of the digital image f can be calculated with the help of a structuring element S and the formula is given as:

$$S\delta*(f))(x) = \max f(x - s)\ s\in S$$

Where x and s represent the vector quantities [12] for the image f. The negative sign in the definition of the dilation represents a counter-intuitive. To avoid this, an alternative is used as follows:

$$(\delta(f))(x) = \max f(x + s)\ s\in S$$

Erosion ε can be computed for the image f at each pixel (x, y) by centering S at (x, y), and then taking the minimum of all pixels in f that are 'hit' by S. Dilation is also computed in the same way, except that the maximum is now considered instead of the minimum. During erosion and dilation padding of values with $-\infty$ and ∞ is considered in order to process the image better.

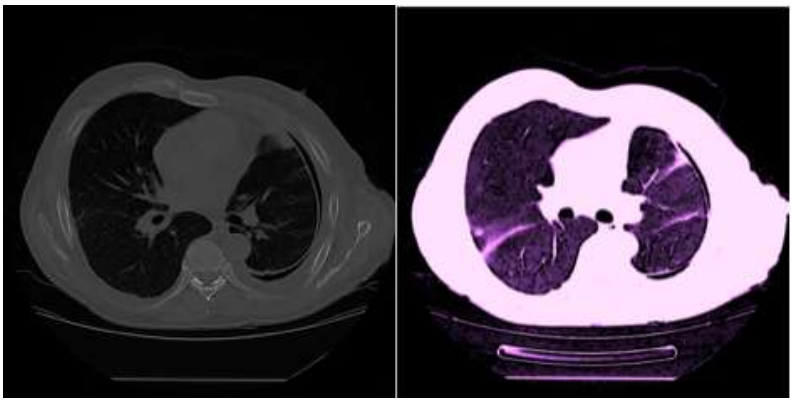

Figure 2: Input image and final output image of the segmented lung

Conclusion. All current segmentation methods of the cardio-vascular system, though they segment images, some of them are very primitive, some cannot identify pathologies and the others are computationally very expensive to perform. When two or three of the above suggested methods are joined together and then carried out, they do provide better results but they are rather time consuming and also expensive.

To segment the lung CT images more effectively, the image first undergoes canny edge detection in which it undergoes five separate processes of filtering to identify the edges of the lung image and to reduce obvious noise. This image is then passed through a median filter to identify the remaining unnecessary noise. The original CT image and the noise are subtracted from each other by comparing and removing matching pixels to provide a lung image with minimal or no noise. This is finally passed through an erosion filter so that remaining unwanted features are removed and only the visible segments of the lung are displayed.

In case of holes or abnormalities in the lungs, blob filtering should also be used with erosion filter to remove the abnormality and preserve the borders.

Works only on CT images where segments of the lungs are clearly seen by the human eye, otherwise segments could be lost.

The research is partially supported by the Grant of the Russian Fund of Basic Research no. 16-47-700289.

REFERENCES

1. Significant savings in radiologic report turnaround time after implementation of a complete picture archiving and communication system (PACS). Twair AA, Torreggiani WC, Mahmud SM, Ramesh N, Hogan B, J Digit Imaging. 2000 Nov; 13(4):175-7.
2. Automatic lung segmentation for accurate quantitation of volumetric X-ray CT images. Hu S, Hoffman EA, Reinhardt JM, IEEE Trans Med Imaging. 2001 Jun; 20(6):490-8.
3. Hierarchical scale-based multiobject recognition of 3-D anatomical structures. Bagci U, Chen X, Udupa JK, IEEE Trans Med Imaging. 2012 Mar; 31(3):777-89.
4. Sonka M, , Hlavac V, , Boyle R.. Image processing, analysis, and machine vision. 3rd ed. Toronto, Ontario: Thomson, 2008.
5. A framework for evaluating image segmentation algorithms. Udupa JK, Leblanc VR, Zhuge Y, Imielinska C, Schmidt H, Currie LM, Hirsch BE, Woodburn J, Comput Med Imaging Graph. 2006 Mar; 30(2):75-87.
6. Canny, J., A Computational Approach To Edge Detection, IEEE Trans. Pattern Analysis and Machine Intelligence, 8(6):679–698, 1986.
7. Chao Wang, Zhongfu Ye, "Salt-and-pepper noise removal by adaptive median filter and TV inpainting," Journal of University of Science and Technology of China, 2008, vol.38, no. 3, pp. 282-287.
8. Tingbiao Chen, Liangzheng Xia, "Digital image processing," Beijing: Posts & Telecommunications Press, 1994.
9. E.R.Davies, Machine vision Theory, Algorithms, Practicalities, Elsevier, 2006.
10. S. Beucher. Segmentation d'Images et Morphologie Math_ematique. PhD thesis, Ecole des Mines, Paris, June 1990.
11. L. Vincent. Graphs and mathematical morphology. Signal Processing, 16:365{388, Apr. 1989.
12. S. R. Sternberg. Parallel architecture for image processing. In 3rd Int. IEEE Compsac, Chicago,
    1979.